

A Peek into the Plasmidome of Global Sewage

Philipp Kirstahler¹, Frederik Teudt¹, Saria Otani¹, Frank M. Aarestrup¹, and Sünje Johanna Pamp^{1*}

¹ Research Group for Genomic Epidemiology, Technical University of Denmark, Kgs. Lyngby, Denmark

1 *Correspondence: sjpa@dtu.dk

2 Technical University of Denmark, 2800 Kongens Lyngby, Denmark.

3

4 **Keywords**

5 Plasmids, microbiome, wastewater, human, animals, Oxford Nanopore Sequencing

6 ***Abstract***

7 Plasmids can provide a selective advantage for microorganisms to survive and adapt to new
8 environmental conditions. Plasmid-encoded traits, such as antimicrobial resistance (AMR) or
9 virulence, impact on the ecology and evolution of bacteria and can significantly influence the burden
10 of infectious diseases. Insight about the identity and functions encoded on plasmids on the global
11 scale are largely lacking. Here we investigate the plasmidome of 24 samples (22 countries, 5
12 continents) from the global sewage surveillance project. We obtained 105 Gbp Oxford Nanopore and
13 167 Gbp Illumina DNA sequences from plasmid DNA preparations and assembled 165,302 contigs
14 (159,322 circular). Of these, 58,429 encoded for genes with plasmid-related and 11,222 with
15 virus/phage-related proteins. About 90% of the circular DNA elements did not have any similarity to
16 known plasmids. Those that exhibited similarity, had similarity to plasmids whose hosts were
17 previously detected in these sewage samples (e.g. *Acinetobacter*, *Escherichia*, *Moraxella*,
18 *Enterobacter*, *Bacteroides*, and *Klebsiella*). Some AMR classes were detected at a higher abundance
19 in plasmidomes (e.g. macrolide-lincosamide-streptogramin B, macrolide, and quinolone), as
20 compared to the respective complex sewage samples. In addition to AMR genes, a range of functions
21 were encoded on the candidate plasmids, including plasmid replication and maintenance,
22 mobilization, and conjugation. In summary, we describe a laboratory and bioinformatics workflow
23 for the recovery of plasmids and other potential extrachromosomal DNA elements from complex
24 microbiomes. Moreover, the obtained data could provide further valuable insight into the ecology and
25 evolution of microbiomes, knowledge about AMR transmission, and the discovery of novel
26 functions.

27

28 ***Importance***

29 This is, to the best of our knowledge, the first study to investigate plasmidomes at a global scale
30 using long read sequencing from complex untreated domestic sewage. Previous metagenomic
31 surveys have detected AMR genes in a variety of environments, including sewage. However, it is
32 unknown whether the AMR genes were encoded on the microbial chromosome or are located on
33 extrachromosomal elements, such as plasmids. Using our approach, we recovered a large number of
34 plasmids, of which most appear novel. We identified distinct AMR genes that were preferentially
35 located on plasmids, potentially contributing to their transmissibility. Overall, plasmids are of great
36 importance for the biology of microorganisms in their natural environments (free-living and host-
37 associated), as well as molecular biology, and biotechnology. Plasmidome collections may therefore
38 be valuable resources for the discovery of fundamental biological mechanisms and novel functions
39 useful in a variety of contexts.

40 ***Introduction***

41 The term plasmid was introduced by Joshua Lederberg in 1952 to describe any extrachromosomal
42 genetic particle (1). It was not until the 1970s when interest in plasmid research rapidly increased and
43 plasmids were introduced as cloning vectors into an area that was dominated by phages as the vector
44 for the transfer of pieces of DNA of choice (2). Since then, plasmids have been highly valuable tools
45 in molecular microbiology. In their natural environment, plasmids are considered key players in
46 horizontal gene transfer. They play crucial roles in the ecology and evolution of bacteria, including
47 their pathogenicity as they can carry virulence factors such as toxins as well as antimicrobial
48 resistance genes (3) (4–6). However, the global diversity of plasmids and distribution of
49 antimicrobial resistance genes are yet to be revealed.

50 The presence of antimicrobial resistance genes on plasmids are of major interest in the clinical and
51 veterinary areas since they can render prescribed antibiotics for treating pathogens ineffective. There
52 have been a range of large-scale metagenomic-based surveys of antimicrobial resistance genes in
53 soils, humans, animals, plants, and sewage (7–12). However, the genomic context of the AMR genes
54 is largely unknown; for example, whether they are located in the bacterial genome or on plasmids.
55 Such knowledge would be of great value to better assess their potential transmissibility rates and
56 global impact of AMR-gene carrying plasmids on human health.

57 Plasmids are usually circular DNA elements in bacterial cells, but they can also occur in linear form
58 and be present in archaea and eukaryotic organisms. The size of plasmids is highly variable, ranging
59 from 1,000 bases to hundreds of kilobases. They are present in different quantities (copy numbers) in
60 bacterial cells, varying from a single copy to hundreds of copies in a single cell. This intrinsic and
61 unique nature of plasmids brings about several challenges in plasmidome research (i.e. research on
62 the collective plasmid content in a sample). For example, the low plasmid/chromosome DNA ratio
63 and potential low copy numbers can make it difficult to detect plasmids. These challenges are
64 amplified when plasmidomes are examined from relatively low-cell-density environments such as
65 wastewater. Even assembling and identifying plasmids with low copy number from high biomass
66 samples including single isolates from whole genome sequencing (WGS) data can be challenging. To
67 address these challenges, different approaches have been developed to increase the recovery of
68 plasmids from WGS data (13–16).

69 Plasmids have now also been recovered from more complex microbiomes using a number of
70 strategies. This includes multiple displacement amplification (MDA) with phi29 DNA polymerase
71 prior to DNA sequencing (17), long read sequencing technology of plasmid DNA, or involvement of
72 advanced assembly strategies (18–21). These studies have however been restricted to a single or few
73 locations, and there is limited knowledge on similarity and differences between plasmids from a

74 range of geographical locations (22–26). We recently showed differences in the AMR gene profiles
75 in urban sewage around the globe, but the location of these AMR genes in the bacteria remains
76 unknown (7).

77 To explore the plasmidome of global sewage, which is characterized by low bacterial cell numbers
78 and challenges to isolate plasmid DNA as previously shown (23–27), we here employ an optimized
79 plasmid DNA isolation procedure, followed by both, plasmid-safe DNase treatment and MDA to
80 obtain sufficient plasmid DNA for Oxford Nanopore sequencing from global urban sewage samples.
81 To improve plasmidome characterizations, we develop an assembly workflow, utilizing the long-read
82 length from the Oxford Nanopore MinION sequencer and Illumina sequences. We obtain thousands
83 of circular candidate plasmid sequences and explore their predicted function.

84

85 ***Material and Methods***

86 ***Sample collection and preparation***

87 From the global sewage sample collection (7), we selected 24 samples from 22 countries (see Table
88 S1 in the supplementary material). The samples originated from the five most populated continents
89 on Earth and for which we had sufficient sample material available. From each sample, a sewage
90 pellet was collected from 250 ml untreated sewage by centrifugation at 10,000xg for 10 minutes at
91 5°C. The sewage pellets were stored at -80°C until use.

92

93 ***Plasmid DNA extraction and enrichment***

94 Plasmid DNA isolation was performed on individual sewage pellets (420 mg) using Plasmid
95 Purification Mini Kit (Qiagen, Cat No./ID: 12123) with QIAGEN-tip 100 (Qiagen, Cat No./ID:
96 10043) following the manufacturer's instruction with the following minor modifications: protein
97 precipitation with P3 buffer mixture was incubated on ice for 15 minutes, elution buffer QF and EB
98 buffer were preheated at 65°C prior to application, and the DNA pellet washing step was done using
99 ice-cold 70% ethanol after isopropanol precipitation. LyseBlue dye for cell lysis indication was
100 added, and all buffer volumes were adjusted to sewage pellet weight. The plasmid DNA pellet was
101 dissolved in 35 µl EB buffer for 1 hour at room temperature. Linear chromosomal DNA was reduced
102 by Plasmid-Safe ATP-Dependent DNase (Epicentre, USA) treatment for 24 hours at 37°C according
103 to the manufacturer's instructions. The DNase was inactivated at 70°C for 30 minutes. To selectively
104 enrich for circular DNA, the plasmid-Safe DNase-treated DNA was amplified using phi29 DNA
105 polymerase (New England Biolabs, USA) following the manufacturer's instructions, similar to as
106 previously described (22). The plasmid DNA is amplified through rolling circle amplification by the
107 phi29 DNA polymerase using random primers, generating multiple DNA replication forks (17). This

108 results in long DNA fragments that contain tandem copies (tandem repeats) of the same plasmid.
109 Blank controls were used during plasmid DNA extractions and plasmid enrichment treatments. All
110 negative controls had undetectable DNA measurements using Qubit double-stranded DNA (dsDNA)
111 BR assay kit on a Qubit 2.0 fluorometer (Invitrogen, Carlsbad, CA).

113 ***Plasmid DNA quality assessment***

114 The plasmid DNA yields from the sewage samples were evaluated using gel electrophoresis and
115 Qubit double-stranded DNA (dsDNA) BR assay kit on a Qubit 2.0 fluorometer (Invitrogen, Carlsbad,
116 CA). Plasmid DNA purity was measured and validated by absorbance ratio of 260/280 and 260/230
117 using NanoDrop 100 (ThermoFisher). During pilot experiments that were aimed at protocol
118 development and plasmid DNA enrichment, we also assessed the quality of our plasmid DNA
119 preparations using a 2100 Bioanalyzer (Agilent).

121 ***Library preparation and Oxford Nanopore sequencing***

122 One μg plasmid DNA in $45\ \mu\text{l}$ buffer was used for library preparation. DNA was used without
123 fragmentation. End repair and dA-tailing were performed using NEBNext FFPE Repair Mix (New
124 England BioLabs, 6630) and NEBNext® Ultra™ II End Repair/dA-Tailing Module (New England
125 BioLabs, 7546). DNA was mixed with $3.5\ \mu\text{l}$ NEBNext FFPE DNA Repair Buffer, $2\ \mu\text{l}$ NEBNext
126 FFPE DNA Repair Mix, $3.5\ \mu\text{l}$ Ultra II End-prep reaction buffer and $3\ \mu\text{l}$ Ultra II End-prep enzyme
127 mix and volume was adjusted to $60\ \mu\text{l}$ with nuclease-free water. The reaction tube was flicked 3
128 times and incubated at 20°C for 10 minutes, then inactivated by heating at 65°C for 10 minutes.
129 Clean-up was done using $60\ \mu\text{l}$ Agencourt AMPure XP beads. The beads-reaction suspension was
130 incubated on a HulaMixer at the lowest speed for 10 minutes, followed by two washes with freshly
131 prepared 70% ethanol. DNA was then eluted from the beads in $61\ \mu\text{l}$ 65°C preheated nuclease-free
132 water. A $1\ \mu\text{l}$ DNA aliquot was assessed with Qubit dsDNA BR assay to ensure $>700\ \text{ng}$ were
133 recovered. A volume of $60\ \mu\text{l}$ of dA-tailed plasmid DNA were added to $25\ \mu\text{l}$ Ligation Buffer (LNB),
134 $10\ \mu\text{l}$ NEBNext Quick T4 DNA Ligase NEBNext Quick Ligation Module (New England BioLabs,
135 6056) and $5\ \mu\text{l}$ Adapter Mix (AMX), and mixed by flicking the tube 3-4 times followed by incubation
136 at room temperature for an extended time of 1 hr. The adaptor-ligated plasmid DNA was cleaned up
137 by adding $40\ \mu\text{l}$ Agencourt AMPure XP beads, and the reaction was mixed by flicking the tube and
138 followed by incubation on a HulaMixer at the lowest speed for 10 minutes. The beads were pelleted
139 and resuspended twice in $250\ \mu\text{l}$ Long Fragment Buffer LFB buffer (SQK-LSK109 kit, Oxford
140 Nanopore Technologies). The cleaned adaptor-ligated DNA was then eluted by incubating the pellet
141 in $15\ \mu\text{l}$ Elution Buffer (SQK-LSK109 kit, Oxford Nanopore Technologies) for 20 minutes at room
142 temperature, then transferring the supernatant to a new tube as constructed library. Flowcell priming

143 and library loading preparation were performed according to the manufacturer's instruction (SQK-
144 LSK109 kit, Oxford Nanopore Technologies). Libraries were loaded on FLO-MIN106 R 9.4.1
145 Oxford Nanopore flowcells, and sequencing was run for 48 hours with MinKNOW software default
146 settings.

147

148 ***Illumina Sequencing***

149 The enriched plasmid DNA samples were also subjected to Illumina NextSeq sequencing for
150 downstream error-correction of contigs. Libraries were prepared using Nextera XT DNA Library
151 Preparation Kit (Illumina, USA) following the manufacturer's instructions. The libraries were
152 sequenced using NextSeq 550 system (Illumina) with 2 X 150 bp paired-end sequencing per flow
153 cell.

154

155 ***Data processing***

156 Basecalling of Nanopore reads was performed using the guppy basecaller (version 3.0.3+7e7b7d0)
157 with the dna_r9.4.1_450bps_hac (high accuracy) configuration. Adapter trimming was performed
158 using porechop (version 0.2.3) downloaded from <https://github.com/rrwick/Porechop> using the
159 default parameters. Illumina sequencing data were quality and adapter trimmed using bbdduk from the
160 bbmap suite (<https://sourceforge.net/projects/bbmap/>, version 38.23) using the following settings:
161 qin=auto, k=19, rref=adapters.txt, mink=11, qtrim=r, trimq=20, minlength=50, tbo, zipllevel=6,
162 overwrite=t, statscolumns=5.

163

164 ***Plasmid assembly from single Nanopore reads***

165 Nanopore reads shorter than 10,000 bases were discarded. Each remaining read was cut into 1,500
166 bases long fragments and passed to the assembly step. The initial fragmentation step of the reads is
167 needed since each read, amplified from a circular element during sample preparation, consists of
168 multiple tandem repeats of the circular element. This is done to eliminate the tandem repeats as well
169 as increase the accuracy of the resulting candidate plasmid DNA sequence. We set the cutting
170 threshold to 1.5 kb to balance between preserving the benefits of long read sequencing and
171 accounting for the error rate of Nanopore sequencing. We decided for a length threshold for cutting
172 (i.e. 1.5 kbp) to not create candidate plasmid DNA sequences from small plasmids that contain
173 multiple copies of the same plasmid. We set the cutting threshold to 1.5 kbp to balance between
174 preserving the benefits of long read sequencing and the error rate of Nanopore sequencing. We also
175 preferred to keeping the cutting threshold more towards the short range to not create candidate
176 plasmids form small plasmids that contain multiple copies of the same plasmid sequence. Read

177 fragments originating from one single read were assembled using minimap2 (version 2.17-r943-dirty)
178 in combination with miniasm version 0.3-r179 (parameter -s 800bp), and error corrected using racon
179 version 1.3.3 (28–30). Assembled contigs were discarded if, after mapping the assembled contig back
180 to the original Nanopore read, hits did not span more than 60% of the read, and if two hits overlapped
181 by more than 50 bp. Assembled candidate contigs were error-corrected using 5 iterations of pilon
182 version 1.23 using the respective Illumina reads from the same sample (31). Candidate contigs longer
183 than 1,000 bases were used for downstream analyses. A schematic overview of the method is
184 presented in Figure 1A.

186 ***Global plasmidome analysis***

187 To examine the obtained plasmids from our global sewage collection in relation to already known
188 plasmids, we compared our obtained candidate plasmid DNA sequences to the DNA sequences in the
189 plasmid database (PLSDB) using the webtool of PLSDB version 2019_10_07 (32). We used search
190 strategy ‘Mash screen’ with a maximum p-value of 0.005 and minimum identity of 95%, as well as
191 the option ‘winner-takes-all strategy. Samples with less than 100 circular assembled contigs were
192 removed from the analysis as well as genera with less than 10 occurrences over all samples. A
193 clustering of samples was performed using Euclidean distance of the clr-transformed values.
194 Furthermore, all candidate plasmid sequences were sketched using MASH version 2.2 (33). The
195 MASH-distances between all samples were calculated using default settings, resulting in a 24 by 24
196 distance table that was used for principal component analysis.

198 ***Antimicrobial resistance gene detection analysis***

199 The trimmed Nanopore and Illumina reads were mapped against the ResFinder database (2020-01-
200 25) using kma (version 1.3.0) (34, 35). The Nanopore reads were mapped with settings: mem_mode,
201 ef, nf, bcNano, and bc=0.7. Illumina reads were mapped with settings: mem_mode, ef, nf, lt1, cge,
202 and t=1. Resistance genes were counted across variants, for example the alleles tet(A)_4_AJ517790
203 and tet(A)_6_AF534183 were both counted as tet(A). Centered log ratios were calculated using the
204 pyCoDa package (<https://bitbucket.org/genomicpidemiology/pycodasrc/master/>).

206 ***Gene prediction and functional analysis***

207 Gene prediction was performed using prodigal version 2.6.3, and annotation of protein families was
208 done using hmmscan from HMMER3 version 3.3.1 (<http://hmmer.org/>) against the pfam database
209 version 33 (36, 37). Predicted genes as well as functional annotation were rejected if the p-value was
210 above 0.000001. Gene ontology (GO) annotations for Pfam IDs were acquired using the mapping of
211 Pfam entries to GO terms as described by Mitchell *et al.* (38).

212 To distinguish between potential plasmid and non-plasmid contigs, we used a scheme described
213 previously (39). The scheme contains Pfam identifiers highly specific for plasmids and viruses.
214 Proteins with a plasmid replication initiator protein Rep_3 (PF01051) domain (n=24,824) were
215 investigated further together with the full set of reference Rep_3-domain proteins (n=1,637)
216 downloaded from Pfam (version 33.1). The two data sets were combined and Rep_3-domain proteins
217 with a length of <40 aa residues were discarded, resulting in a data set of 16,930 Rep_3 (PF01051)
218 domain proteins. The protein sequences were aligned using MAFFT (version 7.221) as part of the
219 Galaxy platform (40, 41). A phylogenetic tree was then build using FastTree (version 2.1.10) (42)
220 and visualized using FigTree (version 1.4.4) (<https://github.com/rambaut/figtree/releases>).

221

222 *Generation of plasmid maps*

223 The 50 longest assemblies from each sample were annotated using Prokka (43). Contigs of interest
224 were chosen for mapping based on the presence of known plasmid-encoded genes, such as replication
225 and mobilization systems, toxin-antitoxin pairs, and AMR genes. Plasmids were inspected and
226 visualized using DNAPlotter (44) and Geneious Prime version 2020.2.4 (www.geneious.com). If a
227 coding sequence (CDS) from the Prokka analysis remained unannotated, it was manually annotated
228 by using BLAST search function against the nr database (45) and scanned with HMMER3 against the
229 Pfam database as described above.

230

231

232 **Results**

233 ***Nanopore and Illumina sequencing output from plasmid DNA-enriched global sewage*** 234 ***samples***

235 The sequencing of 24 plasmid-enriched DNA preparations from untreated sewage from 5 continents
236 (Africa, Asia, Europe, North America, and South America) using Oxford Nanopore sequencing
237 technology produced 1.2 to 9.7 Gbp (median 3.5 Gbp) sequencing data per sample (see Table S1 in
238 the supplementary material). The median read length was 7.3 kb (range 1,075 to 11,018 bases) (see
239 Figure S1 in the supplemental material). After quality trimming and removing sequences below
240 10,000 bases, the median sequencing throughput was 1.9 Gbp and the median read length 23,000
241 bases (see Table A at <https://doi.org/10.6084/m9.figshare.13395446>). The Illumina generated
242 sequencing data per sample were between 1.5 and 9.7 Gbp with a median of 4.8 Gbp after adapter
243 and quality trimming. A median of 41 million paired-end reads per sample were obtained (see Table
244 B at <https://doi.org/10.6084/m9.figshare.13395446>).

246 ***Circular DNA sequences obtained using single Oxford Nanopore reads***

247 Upon assembly and polishing (Figure 1A), we obtained a total of 165,302 contigs from the 24
248 sewage samples, of which 159,322 contigs (96.4%) were suggested by miniasm to be circular (Figure
249 1B, and see Table C at <https://doi.org/10.6084/m9.figshare.13395446>). The longest assembled
250 circular contig had a length of 17.4 kbp and was obtained from a sample in Brasil (BRA.1, South
251 America). Most of the circular contigs were obtained from the Tanzanian (TZA, Africa) sewage
252 sample, and they had an average length of 1.7 kbp (see Table C at
253 <https://doi.org/10.6084/m9.figshare.13395446>).

255 ***Classification of assembled circular DNA elements***

256 To obtain information about the identity of the obtained circular DNA elements, we performed gene
257 prediction, annotation, and classification based on plasmid- and virus/phage-specific Pfam domains
258 (39). Overall, we detected Pfam domains (including domains of unknown function (DUF)) on
259 47.01% of the circular elements, potentially suggesting the presence of many novel DNA sequences
260 not encoding for known protein domains. For the DNA elements (circular & linear) for which Pfam
261 domains were detected, the majority (88.39%) contained predicted genes with plasmid- or
262 virus/phage-related Pfam entries (see Figure 2, Figure S2 in the supplementary material, and Table D
263 at <https://doi.org/10.6084/m9.figshare.13395446>). Overall, we found 55,337 circular DNA elements
264 that encoded for known plasmid-related Pfam domains (and not viral-related Pfam domains). The
265 highest number of plasmid-related candidate sequences were detected in the sample from the Czech

266 Republic (CZE, Europe), followed by Tanzania (TZA, Africa), and Kosovo (XK, Europe). The
267 sample from China (CHN, Asia) was the only sample from which more potential virus/phage-related
268 contigs than candidate plasmids were obtained (see Figure 2, Figure S2 in the supplementary
269 material, and Table D at <https://doi.org/10.6084/m9.figshare.13395446>).

270 On the circular elements with plasmid-related Pfam domains, protein families involved in plasmid
271 replication were the most abundant and they included Relaxase, *Rep_1*, *Rep_2*, *Rep_3*, *Rep_trans*,
272 *RepL*, and *Replicase* (Figure 2A). For example, we detected a total of 24,824 open reading frames
273 with a plasmid replication initiator protein *Rep_3* (PF01051) domain. Even though *Rep_3*-domain
274 proteins from all continents were observed across the phylogenetic tree, some clades mainly
275 represented proteins from one continent, interspersed with protein sequences from other continents
276 (Figure 2B). For instance, clades that mainly harbored proteins originating from Europe, also
277 frequently contained protein sequences from North America and other continents. Clades dominated
278 by *Rep_3* (PF01051) domain proteins from Africa also frequently harbored similar proteins from
279 South America.

280 Furthermore, protein families involved in plasmid mobilization were detected, such as *Mob_Pre*,
281 *MobA_MobL*, and *MobC* (Figure 2A). In addition, we identified protein families related to
282 virus/phage replication and capsid proteins, as well as protein domains binding to DNA (*HTH_17*,
283 *HTH_23*, *HTH_Crp_2*) and that might be involved in regulating gene expression.

285 ***Global plasmidome pattern based on known plasmids***

286 To examine whether our collection of plasmid sequences contained already known sequences, we
287 compared the obtained plasmid DNA sequences to the entries in the plasmid database (PLSDB). This
288 analysis revealed that only 10.1% of our circular elements were similar to known plasmids (see Table
289 E at <https://doi.org/10.6084/m9.figshare.13395446>). The majority of plasmids that exhibited some
290 similarity to entries in the PLDB originated from *Acinetobacter* (33%), *Enterococcus* (21%) as well
291 as *Flavobacterium* (10%); genera that were previously detected in these sewage microbiomes (7).

292 Overall, most plasmids with similarities to already known ones were found in the samples from India,
293 Kosovo, Pakistan, Czech Republic, Iceland, and Brazil (see Table E at
294 <https://doi.org/10.6084/m9.figshare.13395446>). Clustering analysis of the abundancies of plasmids
295 with known relatives in PLSDB revealed three main clusters (Figure 3A). The first cluster comprised
296 samples that overall exhibited a low number of known plasmids and included samples from Europe
297 (ALB, POL, ESP, SVN) and a sample from Ghana. The second cluster included samples with
298 plasmids from a large range of bacterial genera at higher abundance, and comprised samples from
299 Europe (ISL, DEU, CZE), North America (USA.1, USA.2, CAN), India, Brazil and Tanzania. The
300 third cluster comprised samples with known plasmids from few bacterial genera and included

301 samples from Asia (CHN, PAK), Africa (CIV), Europe (XK), and South America (ECU, PER)
302 (Figure 3A).
303 In a principal component analysis of the same data, a similar clustering was observed. Furthermore,
304 along the first principal component, samples from Asia and Europe appeared to be most different
305 from each other and with samples from Africa, and North and South America in between. Upon
306 examining the particular reference plasmids and their bacterial hosts that were driving this pattern a
307 similar observation was made: plasmids from bacterial hosts originating from Europe appeared to
308 segregate along the first principle component from plasmids and their bacterial hosts originating from
309 Asia (Figure 3B). This observation was supported by a cluster analysis on plasmid-level, in which
310 five clusters were observed: Samples from Europe did not cluster with samples from Asia, and
311 different sets of known plasmids were found in the samples from Europe and Asia, respectively (see
312 Figure S3 in the supplemental material). Generally, only few known plasmids were detected in the
313 samples from Albania, Slovenia, Spain, Poland, Ecuador, and Ghana (see Figure S3 in the
314 supplementary material and Table E at <https://doi.org/10.6084/m9.figshare.13395446>).
315 Given the large fraction of candidate plasmid sequences that did not exhibit similarity to already
316 known plasmids, we performed a reference-independent analysis by calculating Mash-distances
317 based on all plasmid sequences for each sample. In this analysis, the plasmidomes clustered in two
318 main clusters (see Figure S4 in the supplemental material). The first cluster harbored all samples
319 from Europe (with the exception of Poland), as well as the samples from Canada (North America),
320 Pakistan and India (Asia), and Côte d'Ivoire (Africa). The second cluster harbored all samples from
321 South America, both samples from the USA (North America), as well as Tanzania and Ghana
322 (Africa), and China (Asia) (see Figure S4 in the supplemental material). This suggests that the
323 sequence space encompassing novel plasmid sequences (i.e. those that did not exhibit similarity to
324 sequences in the PLSDB) provides an extended, yet to be discovered, dimension into plasmid
325 ecology and evolution.

326 327 ***Antimicrobial resistance genes in plasmidomes***

328 To gain insight into antimicrobial resistance genes on the plasmids from sewage, and compare them
329 to those detected in the whole community of the same sewage samples, we performed a ResFinder
330 analysis on three sequencing read data sets: whole community DNA sequenced using Illumina (7),
331 plasmidome DNA sequenced using Illumina (this study), and plasmidome DNA sequenced using
332 Nanopore sequencing (this study).

333 Overall, many of the antimicrobial resistance genes and antimicrobial classes that were detected
334 using whole community sequencing, were also detected in the two plasmidome datasets, with a few
335 exceptions. For example, the two antimicrobial classes macrolide-streptogramin B and lincosamide-

336 pleuromutilin-streptogramin A were not detected in the plasmidome samples in about half of the
337 cases (Figure 4A, and see Figure S5A in the supplementary material, and Tables F and G at
338 <https://doi.org/10.6084/m9.figshare.13395446>). Occasionally, also genes conferring resistance to
339 other antimicrobial classes were not detected in individual plasmidome samples as compared to the
340 whole community, and these included genes conferring resistance to lincosamide, phenicol, or
341 aminoglycoside. It may be that genes that were detected more frequently in the whole community
342 sample, as compared to the plasmidome samples, are preferentially encoded on the bacterial
343 chromosomes or larger plasmids.

344 Conversely, genes conferring resistance to the antimicrobial classes macrolide-lincosamide-
345 streptogramin B, as well as macrolide, and quinolone, were more frequently observed in the
346 plasmidome samples (Figure 4A, and see Figure S5 in the supplementary material and Tables F and
347 G at <https://doi.org/10.6084/m9.figshare.13395446>). The most frequently observed AMR genes
348 related to these three classes were *ermB*, *ermT*, *ermF* (macrolide-lincosamide-streptogramin B),
349 *mphE*, *mefA*, *msrD* (Macrolide), and *qnrB19*, *qnrD1*, *qnrD2*, *qnrD3*, *qnrVC4* (Quinolone). The
350 higher frequency of those genes in the plasmidome samples may suggest that they are more
351 frequently found on plasmids in general, or on smaller plasmids as compared to large ones. Another
352 gene that was frequently observed across samples is *msrE*, and which was slightly higher abundant in
353 plasmidomes (average abundance 15.4%, SEM 1.86) as compared to whole community samples
354 (average abundance 11.5%, SEM 1.88). As examples, a few randomly chosen candidate plasmids and
355 their encoded genes, including AMR genes, are displayed in Figure 4B.

357 ***Functional characterization of plasmidomes***

358 To gain further insight into the functions encoded on all circular elements, we obtained GO
359 annotations for the predicted proteins through mapping of pfam entries to GO terms. A clustering
360 analysis revealed the separation of plasmidomes into two main clusters (see Figure S6 in the
361 supplemental material). Cluster 1 comprised samples from Europe (ISL, CZE, XK, DEU) as well as
362 North America (USA.1, CAN) and South America (BRA.1, ECU). Cluster 2 comprised the samples
363 from Asia (IND, PAK, CHN), Africa (TZA, CIV) and the remaining samples from Europe (POL,
364 ESP, SVN) and South America (PER). This clustering based on protein functions appeared to have
365 some similarity to the clustering based on nucleotide sequence similarity to known plasmids (Figure
366 3). In both analyses, the European samples from ISL, CZE, and DEU exhibited similarities, while the
367 other European samples from POL, ESP, SVN clustered together separately. Furthermore, in both
368 analyses, samples from North America (USA.1, CAN) and South America (BRA.1) clustered with
369 the European samples from ISL, CZE, and DEU.

370 Functions that appeared to be enriched in samples from cluster 1 include, conjugation, recombinase
371 activity, DNA methylation, protein secretion (type IV secretion system), response to antibiotic, toxic
372 substance binding, response to toxic substance, unidirectional conjugation, and bacteriocin immunity
373 (see Figure S5 in the supplemental material). Cluster 2 appeared to overall have fewer proteins that
374 could be annotated using this strategy, and the samples exhibited a higher diversity of functional
375 patterns compared to samples from cluster 1. Some samples from cluster 2 exhibited an enrichment
376 of proteins that may be related to viruses/phages, such as viral capsids, structural molecule activity,
377 RNA binding, RNA helicase activity, and these were in particular samples that appeared to have a
378 higher abundance of virus/phage related Pfam domains (Figure 2). The majority of samples in both
379 clusters harbored proteins involved in plasmid maintenance (see Figure S6 in the supplemental
380 material).

382 *Discussion*

383 This is the first study to investigate plasmidomes at a global scale using long read sequencing from
384 sewage. We show that our approach facilitated the recovery of complete plasmids from complex
385 metagenomic samples with a sufficient quality to perform gene prediction and functional annotation.
386 In total, we obtained 165,302 DNA elements of which 159,322 were circular. The average length was
387 1.9 kb (min 1 kbp, max 17.4 kbp), suggesting that mainly small plasmids were obtained. This might
388 reflect the true distribution but could also be biased due to a number of reasons, for example, smaller
389 plasmids are more stable and thus have higher chance of getting through the DNA extraction step
390 undamaged. Since a DNase step was used to reduce the amount of chromosomal DNA, damaged
391 plasmids might have been digested as well. Another possibility could be that some plasmids were
392 already damaged during storage and transportation, as the sewage was frozen and shipped, and many
393 of the samples arrived thawed and were frozen again. Another reason could be that our assembly
394 workflow was not able to perform a successful assembly on larger plasmids with a high number of
395 tandem-repeats.

396
397 We identified a range of functions encoded on the candidate plasmids, including plasmid replication
398 and maintenance, mobilization, conjugation, antimicrobial resistance, and bacteriocin immunity.
399 However, not all plasmid-related DNA elements encoded for a plasmid-replication gene, suggesting
400 that they may not be self-replicating DNA molecules. It should though be noted that also already
401 described plasmids do not necessarily encode for a rep gene using current annotation algorithms.
402 Furthermore, we found that about half of the circular DNA elements did not encode for any known
403 Pfam domains. This could suggest that we detected many novel DNA sequences not encoding for

404 known protein domains. A hypothesis could be that a fraction of the circular DNA elements are novel
405 extrachromosomal elements that are hitherto undescribed and may also originate from various
406 domains of life, including bacteria, archaea, and eukaryotes (46–48). Alternatively, open reading
407 frames might not always have been properly detected because of sequencing errors not corrected in
408 the polishing steps with Nanopore and Illumina reads. This could certainly have contributed to it, as
409 we occasionally observed fragmented genes due to remaining sequencing errors, even after polishing.
410 This challenge may be alleviated with the ongoing improvement of Oxford Nanopore chemistry and
411 basecalling algorithms. Nevertheless, collectively, we obtained 58,429 DNA elements (circular &
412 linear) that encoded for proteins with plasmid-related Pfams, and 17,292 circular DNA elements
413 exhibited sequence similarity to known plasmids, suggesting that we successfully discovered many
414 novel candidate plasmid DNA sequences.

415

416 For candidate plasmids that exhibited some similarities to known plasmids, we found that they
417 originated from bacterial taxa previously detected in these complex sewage samples, such as
418 *Acinetobacter*, *Escherichia*, *Moraxella*, *Enterobacter*, *Bacteroides*, and *Klebsiella* (7). These genera
419 include bacteria that are part of the human gut microbiome and/or opportunistic pathogens. Hence,
420 some of these plasmids might play a role in gut microbial ecology and potential antimicrobial
421 resistance transmission (49, 50). It should be noted, however, that overall, only ~10.1% of our
422 circular elements were similar to known plasmids in the PLSDB, and which may be partly explained
423 by differences in plasmid contents (plasmid average size 1.9 kbp (this study) and 53.2 kbp (PLSDB))
424 (32). In line with this, we observed that the plasmidome samples clustered somewhat differently
425 when all candidate plasmid sequences were taken into account (and not only those that exhibited
426 similarity to known reference plasmids). It will be interesting to investigate our candidate plasmids
427 further in future studies, ideally through involvement of more plasmidome samples and extended
428 metadata. There may be a range of factors that may play role in explaining differences and
429 similarities between plasmidomes, such as climate, population-related differences including human
430 ethnicity, health status, sanitation, and economy including trading between countries.

431

432 Overall, AMR classes that were detected in the plasmidome sequencing data sets were also found in
433 the sequencing data from the whole complex sewage samples, suggesting that the plasmidomes are a
434 good representation of what is present in the complex samples. Some AMR gene classes, however,
435 were more predominant in the whole community (e.g. macrolide-streptogramin B, lincosamide-
436 pleuromutilin-streptogramin A), and others more in the plasmidomes (e.g. macrolide-lincosamide-
437 streptogramin B, macrolide, and quinolone). This could suggest that the AMR genes conferring
438 resistance to the latter AMR gene classes are preferentially located on plasmids as compared to

439 chromosomes. However, given that we mainly recovered small plasmids, it could also be an
440 indication for that the AMR genes preferentially detected in the whole community may be located on
441 large plasmids that were not recovered here. Whether certain abundant AMR genes in the
442 plasmidomes are plasmid- or chromosome-associated may also be dependent on the particular
443 bacterial host (see Figure S7 in the supplemental material) (51).

444
445 While our approach and findings are a significant advancement to previous work, there are still
446 aspects that can be improved in the future. For example, the assembly workflow could be improved
447 to resolve remaining repetitive regions within the plasmid, as a range of circular elements still
448 consisted of tandem-repeats of the actual plasmid sequence. This could potentially be solved by
449 introducing a dynamic cutting step using the k-mer composition of the full read. Despite the high
450 error rate of the Nanopore sequencing reads, the raw read should still contain a set of k-mers with 10-
451 15 bases length that could help interfering the appropriate fragmentation length. In addition, the
452 plasmid DNA isolation could be improved significantly to increase a) the overall amount of plasmid
453 DNA (in order to avoid having to perform MDA), and b) the amount of larger plasmids. Further
454 possibilities to identify new plasmids could also involve *in vivo* proximity-ligation Hi-C or single-cell
455 sequencing that would also allow the discovery of new plasmids directly together with their host cell
456 (52, 53).

457
458 Overall, our study provides new insight about the technical applicability of long-read Nanopore
459 sequencing for plasmidome analysis of complex biological samples, as well as a foundation for
460 exploring plasmid ecology and evolution at a global scale. For example, we can now better explore
461 the genomic context of AMR genes, and reveal whether they are located on the microbial
462 chromosome or on mobile genetic elements such as plasmids. This knowledge is of great value in
463 assessing the potential transmissibility of AMR genes with resulting impact on antibiotic treatments
464 in the medical and veterinary sectors and the one health perspective. Furthermore, the dataset
465 provides a valuable resource for further exploring extrachromosomal DNA elements including
466 potential novel functions.

467 468 ***Acknowledgment***

469 This work was mainly supported by The Novo Nordisk Foundation (NNF16OC0021856: Global
470 Surveillance of Antimicrobial Resistance), and partially by the European Union's Horizon 2020
471 Research and Innovation Programme under grant agreement No 773830: One Health European Joint

472 Programme. The funders had no role in study design, data collection and interpretation, or the
473 decision to submit the work for publication.

474 We thank Christina Aaby Svendsen (Technical University of Denmark) for technical support with the
475 Illumina sequencing of the plasmidomes.

476 Sequencing data analysis was performed using the DeiC National Life Science Supercomputer at
477 DTU.

478

479 ***Data availability***

480 The DNA sequences generated in this project are available through ENA/GenBank/DDBJ under the
481 accession number PRJEB41171 (Nanopore reads: ERX4715074-ERX4715097; Illumina reads:

482 ERX5299122-ERX5299145; Assemblies: ERZ1694234-ERZ1694257). The code for the creation of
483 assemblies is accessible from Github (<https://github.com/philDTU/plasmidPublication>) and

484 additional supplementary material is available at

485 https://figshare.com/projects/A_Peek_into_the_Plasmidome_of_Global_Sewage/94448.

486

487 **References**

- 488
- 489 1. Lederberg J. 1952. Cell Genetics and Hereditary Symbiosis. *Physiological Reviews* 32:403–430.
- 490 2. Cohen SN, Chang ACY, Boyer HW, Helling RB. 1973. Construction of Biologically Functional Bacterial
491 Plasmids In Vitro. *PNAS* 70:3240–3244.
- 492 3. Rodríguez-Beltrán J, DelaFuente J, León-Sampedro R, MacLean RC, San Millán Á. 2021. Beyond
493 horizontal gene transfer: the role of plasmids in bacterial evolution. *Nature Reviews Microbiology*
494 <https://doi.org/10.1038/s41579-020-00497-1>.
- 495 4. Johnson TJ, Nolan LK. 2009. Pathogenomics of the Virulence Plasmids of *Escherichia coli*. *Microbiol Mol*
496 *Biol Rev* 73:750–774.
- 497 5. Bratu S, Brooks S, Burney S, Kochar S, Gupta J, Landman D, Quale J. 2007. Detection and Spread of
498 *Escherichia coli* Possessing the Plasmid-Borne Carbapenemase KPC-2 in Brooklyn, New York. *Clin Infect*
499 *Dis* 44:972–975.
- 500 6. Tian G-B, Doi Y, Shen J, Walsh TR, Wang Y, Zhang R, Huang X. 2017. MCR-1-producing *Klebsiella*
501 *pneumoniae* outbreak in China. *The Lancet Infectious Diseases* 17:577.
- 502 7. Hendriksen RS, Munk P, Njage P, Bunnik B, McNally L, Lukjancenko O, Röder T, Nieuwenhuijse D,
503 Pedersen SK, Kjeldgaard J, Kaas RS, Clausen PTLC, Vogt JK, Leekitcharoenphon P, Schans MGM, Zuidema
504 T, Husman AMR, Rasmussen S, Petersen B, Bego A, Rees C, Cassar S, Coventry K, Collignon P,
505 Allerberger F, Rahube TO, Oliveira G, Ivanov I, Vuthy Y, Sopheak T, Yost CK, Ke C, Zheng H, Baisheng L,
506 Jiao X, Donado-Godoy P, Coulibaly KJ, Jergović M, Hrenovic J, Karpíšková R, Villacis JE, Legesse M,
507 Eguale T, Heikinheimo A, Malania L, Nitsche A, Brinkmann A, Saba CKS, Kocsis B, Solymosi N,
508 Thorsteinsdottir TR, Hatha AM, Alebouyeh M, Morris D, Cormican M, O'Connor L, Moran-Gilad J, Alba
509 P, Battisti A, Shakenova Z, Kiiyukia C, Ng'eno E, Raka L, Avsejenko J, Bērziņš A, Bartkevics V, Penny C,
510 Rajandas H, Parimannan S, Haber MV, Pal P, Jeunen G-J, Gemmell N, Fashae K, Holmstad R, Hasan R,
511 Shakoor S, Rojas MLZ, Wasyl D, Bosevska G, Kochubovski M, Radu C, Gassama A, Radosavljevic V,

- 512 Wuertz S, Zuniga-Montanez R, Tay MYF, Gavačová D, Pastuchova K, Truska P, Trkov M, Esterhuyse K,
513 Keddy K, Cerdà-Cuéllar M, Pathirage S, Norrgren L, Örn S, Larsson DGJ, Van der Heijden T, Kumburu HH,
514 Sanneh B, Bidjada P, Njanpop-Lafourcade B-M, Nikiema-Pessinaba SC, Levent B, Meschke JS, Beck NK,
515 Van CD, Do Phuc N, Tran DMN, Kwenda G, Tabo D, Wester AL, Cuadros-Orellana S, Amid C, Cochrane G,
516 Sicheritz-Ponten T, Schmitt H, Alvarez JRM, Aidara-Kane A, Pamp SJ, Lund O, Hald T, Woolhouse M,
517 Koopmans MP, Vigre H, Petersen TN, Aarestrup FM. 2019. Global monitoring of antimicrobial resistance
518 based on metagenomics analyses of urban sewage. *Nature Communications* 10:1124.
- 519 8. Munk P, Knudsen BE x000E6 r, Lukjacenko O, Duarte ASR, Gompel L, Luiken REC, Smit LAM, Schmitt H,
520 Garcia AD, Hansen RB, Petersen TN, Bossers A, x000E9 ER, Graveland H, van Essen A, Gonzalez-Zorn B,
521 Moyano G, Sanders P, Chauvin C, David J, Battisti A, Caprioli A, Dewulf J, Blaha T, Wadepohl K, Brandt
522 M, Wasyl D, ska MS x00144, Zajac M, Daskalov H, Saatkamp HW, rk KDCS x000E4, Lund O, Hald T, Pamp
523 S x000FC nje J, Vigre H x000E5 kan, Heederik D, Wagenaar JA, Mevius D, Aarestrup FM. 2018.
524 Abundance and diversity of the faecal resistome in slaughter pigs and broilers in nine European
525 countries. *Nature Microbiology* 1–14.
- 526 9. Campbell TP, Sun X, Patel VH, Sanz C, Morgan D, Dantas G. 2020. The microbiome and resistome of
527 chimpanzees, gorillas, and humans across host lifestyle and geography. 6. *The ISME Journal* 14:1584–
528 1599.
- 529 10. Chen Q-L, Cui H-L, Su J-Q, Penuelas J, Zhu Y-G. 2019. Antibiotic Resistomes in Plant Microbiomes.
530 *Trends in Plant Science* 24:530–541.
- 531 11. Forsberg KJ, Patel S, Gibson MK, Lauber CL, Knight R, Fierer N, Dantas G. 2014. Bacterial phylogeny
532 structures soil resistomes across habitats. 7502. *Nature* 509:612–616.
- 533 12. Carr VR, Witherden EA, Lee S, Shoaie S, Mullany P, Proctor GB, Gomez-Cabrero D, Moyes DL. 2020.
534 Abundance and diversity of resistomes differ between healthy human oral cavities and gut. 1. *Nature*
535 *Communications* 11:693.

- 536 13. Wick RR, Judd LM, Gorrie CL, Holt KE. 2017. Unicycler: Resolving bacterial genome assemblies from
537 short and long sequencing reads. *PLOS Computational Biology* 13:e1005595.
- 538 14. Antipov D, Hartwick N, Shen M, Raiko M, Lapidus A, Pevzner PA. 2016. plasmidSPAdes: assembling
539 plasmids from whole genome sequencing data. *Bioinformatics* 32:3380–3387.
- 540 15. Vielva L, de Toro M, Lanza VF, de la Cruz F. 2017. PLACNETw: a web-based tool for plasmid
541 reconstruction from bacterial genomes. *Bioinformatics* 33:3796–3798.
- 542 16. Rozov R, Brown Kav A, Bogumil D, Shterzer N, Halperin E, Mizrahi I, Shamir R. 2017. Recycler: an
543 algorithm for detecting plasmids from de novo assembly graphs. *Bioinformatics* 33:475–482.
- 544 17. Dean FB, Nelson JR, Giesler TL, Lasken RS. 2001. Rapid Amplification of Plasmid and Phage DNA Using
545 Phi29 DNA Polymerase and Multiply-Primed Rolling Circle Amplification. *Genome Res* 11:1095–1099.
- 546 18. Che Y, Xia Y, Liu L, Li A-D, Yang Y, Zhang T. 2019. Mobile antibiotic resistome in wastewater treatment
547 plants revealed by Nanopore metagenomic sequencing 1–13.
- 548 19. Bertrand D, Shaw J, Kalathiyappan M, Ng AHQ, Kumar MS, Li C, Dvornicic M, Soldo JP, Koh JY, Tong C,
549 Ng OT, Barkham T, Young B, Marimuthu K, Chng KR, Sikic M, Nagarajan N. 2019. Hybrid metagenomic
550 assembly enables high-resolution analysis of resistance determinants and mobile elements in human
551 microbiomes. *Nature Biotechnology* 1–15.
- 552 20. Antipov D, Raiko M, Lapidus A, Pevzner PA. 2019. Plasmid detection and assembly in genomic and
553 metagenomic datasets. *Genome Res* gr.241299.118.
- 554 21. Jørgensen TS, Hansen MA, Xu Z, Tabak MA, Sørensen SJ, Hansen LH. 2017. Plasmids, Viruses, And Other
555 Circular Elements In Rat Gut. *bioRxiv* 143420.
- 556 22. Kav AB, Sasson G, Jami E, Doron-Faigenboim A, Benhar I, Mizrahi I. 2012. Insights into the bovine rumen
557 plasmidome. *PNAS* 109:5452–5457.

- 558 23. Kav AB, Rozov R, Bogumil D, Sørensen SJ, Hansen LH, Benhar I, Halperin E, Shamir R, Mizrahi I. 2020.
559 Unravelling plasmidome distribution and interaction with its hosting microbiome. *Environmental*
560 *Microbiology* 22:32–44.
- 561 24. Zhang T, Zhang X-X, Ye L. 2011. Plasmid Metagenome Reveals High Levels of Antibiotic Resistance
562 Genes and Mobile Genetic Elements in Activated Sludge. *PLOS ONE* 6:e26041.
- 563 25. Sentchilo V, Mayer AP, Guy L, Miyazaki R, Green Tringe S, Barry K, Malfatti S, Goessmann A, Robinson-
564 Rechavi M, van der Meer JR. 2013. Community-wide plasmid gene mobilization and selection. 6. *The*
565 *ISME Journal* 7:1173–1186.
- 566 26. Kothari A, Wu Y-W, Chandonia J-M, Charrier M, Rajeev L, Rocha AM, Joyner DC, Hazen TC, Singer SW,
567 Mukhopadhyay A. 2019. Large Circular Plasmids from Groundwater Plasmidomes Span Multiple
568 Incompatibility Groups and Are Enriched in Multimetal Resistance Genes. *mBio* 10.
- 569 27. Kav AB, Sasson G, Jami E, Doron-Faigenboim A, Benhar I, Mizrahi I. 2012. Insights into the bovine rumen
570 plasmidome. *PNAS* 109:5452–5457.
- 571 28. Li H. 2018. Minimap2: pairwise alignment for nucleotide sequences. *Bioinformatics* 34:3094–3100.
- 572 29. Li H. 2016. Minimap and miniasm: fast mapping and de novo assembly for noisy long sequences.
573 *Bioinformatics* 32:2103–2110.
- 574 30. Vaser R, Sović I, Nagarajan N, Šikić M. 2017. Fast and accurate de novo genome assembly from long
575 uncorrected reads. *Genome Res* 27:737–746.
- 576 31. Walker BJ, Abeel T, Shea T, Priest M, Abouelliel A, Sakthikumar S, Cuomo CA, Zeng Q, Wortman J, Young
577 SK, Earl AM. 2014. Pilon: An Integrated Tool for Comprehensive Microbial Variant Detection and
578 Genome Assembly Improvement. *PLOS ONE* 9:e112963.
- 579 32. Galata V, Fehlmann T, Backes C, Keller A. 2019. PLSDb: a resource of complete bacterial plasmids.
580 *Nucleic Acids Res* 47:D195–D202.

- 581 33. Ondov BD, Treangen TJ, Melsted P, Mallonee AB, Bergman NH, Koren S, Phillippy AM. 2016. Mash: fast
582 genome and metagenome distance estimation using MinHash. *Genome Biology* 17:132.
- 583 34. Zankari E, Hasman H, Cosentino S, Vestergaard M, Rasmussen S, Lund O, Aarestrup FM, Larsen MV.
584 2012. Identification of acquired antimicrobial resistance genes. *Journal of Antimicrobial Chemotherapy*
585 67:2640–2644.
- 586 35. Clausen PTLC, Aarestrup FM, Lund O. 2018. Rapid and precise alignment of raw reads against
587 redundant databases with KMA. *BMC Bioinformatics* 19:307.
- 588 36. Hyatt D, Chen G-L, Locascio PF, Land ML, Larimer FW, Hauser LJ. 2010. Prodigal: prokaryotic gene
589 recognition and translation initiation site identification. *BMC Bioinformatics* 11:11:119.
- 590 37. El-Gebali S, Mistry J, Bateman A, Eddy SR, Luciani A, Potter SC, Qureshi M, Richardson LJ, Salazar GA,
591 Smart A, Sonnhammer ELL, Hirsh L, Paladin L, Piovesan D, Tosatto SCE, Finn RD. 2019. The Pfam protein
592 families database in 2019. *Nucleic Acids Res* 47:D427–D432.
- 593 38. Mitchell A, Chang H-Y, Daugherty L, Fraser M, Hunter S, Lopez R, McAnulla C, McMenamin C, Nuka G,
594 Pesseat S, Sangrador-Vegas A, Scheremetjew M, Rato C, Yong S-Y, Bateman A, Punta M, Attwood TK,
595 Sigrist CJA, Redaschi N, Rivoire C, Xenarios I, Kahn D, Guyot D, Bork P, Letunic I, Gough J, Oates M, Haft
596 D, Huang H, Natale DA, Wu CH, Orengo C, Sillitoe I, Mi H, Thomas PD, Finn RD. 2015. The InterPro
597 protein families database: the classification resource after 15 years. *Nucleic Acids Res* 43:D213–D221.
- 598 39. Jørgensen TS, Hansen MA, Xu Z, Tabak MA, Sørensen SJ, Hansen LH. 2017. Plasmids, Viruses, And Other
599 Circular Elements In Rat Gut. *bioRxiv* 143420.
- 600 40. Katoh K, Standley DM. 2013. MAFFT Multiple Sequence Alignment Software Version 7: Improvements
601 in Performance and Usability. *Molecular Biology and Evolution* 30:772–780.
- 602 41. Afgan E, Baker D, Batut B, van den Beek M, Bouvier D, Čech M, Chilton J, Clements D, Coraor N, Grüning
603 BA, Guerler A, Hillman-Jackson J, Hiltemann S, Jalili V, Rasche H, Soranzo N, Goecks J, Taylor J,

- 604 Nekrutenko A, Blankenberg D. 2018. The Galaxy platform for accessible, reproducible and collaborative
605 biomedical analyses: 2018 update. *Nucleic Acids Research* 46:W537–W544.
- 606 42. Price MN, Dehal PS, Arkin AP. 2010. FastTree 2 – Approximately Maximum-Likelihood Trees for Large
607 Alignments. *PLOS ONE* 5:e9490.
- 608 43. Seemann T. 2014. Prokka: rapid prokaryotic genome annotation. *Bioinformatics* 30:2068–2069.
- 609 44. Carver T, Thomson N, Bleasby A, Berriman M, Parkhill J. 2009. DNAPlotter: circular and linear
610 interactive genome visualization. *Bioinformatics* 25:119–120.
- 611 45. Altschul SF, Gish W, Miller W, Myers EW, Lipman DJ. 1990. Basic local alignment search tool. *Journal of*
612 *molecular biology* 215:403–410.
- 613 46. Lanciano S, Carpentier M-C, Llauro C, Jobet E, Robakowska-Hyzorek D, Lasserre E, Ghesquière A,
614 Panaud O, Mirouze M. 2017. Sequencing the extrachromosomal circular mobilome reveals
615 retrotransposon activity in plants. *PLOS Genetics* 13:e1006630.
- 616 47. Shibata Y, Kumar P, Layer R, Willcox S, Gagan JR, Griffith JD, Dutta A. 2012. Extrachromosomal
617 microDNAs and chromosomal microdeletions in normal tissues. *Science* 336:82–86.
- 618 48. Møller HD, Mohiyuddin M, Prada-Luengo I, Sailani MR, Halling JF, Plomgaard P, Maretty L, Hansen AJ,
619 Snyder MP, Pilegaard H, Lam HYK, Regenber B. 2018. Circular DNA elements of chromosomal origin
620 are common in healthy human somatic tissue. 1. *Nature Communications* 9:1069.
- 621 49. San Millan A. 2018. Evolution of Plasmid-Mediated Antibiotic Resistance in the Clinical Context. *Trends*
622 *in Microbiology* 26:978–985.
- 623 50. Ogilvie LA, Firouzmand S, Jones BV. 2012. Evolutionary, ecological and biotechnological perspectives on
624 plasmids resident in the human gut mobile metagenome. *Bioengineered* 3:13–31.

- 625 51. Alcock BP, Raphenya AR, Lau TTY, Tsang KK, Bouchard M, Edalatmand A, Huynh W, Nguyen A-LV, Cheng
626 AA, Liu S, Min SY, Miroshnichenko A, Tran H-K, Werfalli RE, Nasir JA, Oloni M, Speicher DJ, Florescu A,
627 Singh B, Faltyn M, Hernandez-Koutoucheva A, Sharma AN, Bordeleau E, Pawlowski AC, Zubyk HL,
628 Dooley D, Griffiths E, Maguire F, Winsor GL, Beiko RG, Brinkman FSL, Hsiao WWL, Domselaar GV,
629 McArthur AG. 2020. CARD 2020: antibiotic resistome surveillance with the comprehensive antibiotic
630 resistance database. *Nucleic Acids Res* 48:D517–D525.
- 631 52. Stalder T, Press MO, Sullivan S, Liachko I, Top EM. 2019. Linking the resistome and plasmidome to the
632 microbiome. *10. The ISME Journal* 13:2437–2446.
- 633 53. Lan F, Demaree B, Ahmed N, Abate AR. 2017. Single-cell genome sequencing at ultra-high- throughput
634 with microfluidic droplet barcoding. *Nature Biotechnology* 35:640–646.

635

636

637 ***Figure legends***

638
639 **Figure 1. Schematic overview of the single read assembly workflow and size distribution of**

640 **assembled reads.** A) Nanopore reads (based on plasmid DNA amplified with phi29) longer than
641 10,000 bases were split into 1,500 bases long fragments. The sequence fragments were then
642 assembled using minimap2 and miniasm and subsequently polished two times: 1. with the Nanopore
643 fragments using racon and 2. with the Illumina reads using pilon. B) The size distribution of circular
644 (orange) and linear (violet) assembled elements. These are the candidate plasmid sequences that
645 successfully mapped to the original Nanopore read (i.e. covering more than 60% of the read, and not
646 overlapping by more than 50 bp for multiple hits). Of the total 165,302 assemblies, 159,322 were
647 characterized to be circular and 5,980 to be linear.

648
649 **Figure 2. Functional characterization of circular DNA elements based on protein families.** A)

650 The bar plot displays the fraction of Pfam identifiers assigned to predicted proteins on the circular
651 elements. The 31 Pfam identifiers represent the Top10 Pfam identifiers for each sample. Protein
652 domains specifically involved in plasmid mobilization and plasmid replication are indicated by red
653 and blue colors, respectively (see legend to the bottom right). Virus/phage related Pfam identifiers
654 are indicated in green colors. Remaining Pfam identifiers are grouped (other) and indicated by dark
655 grey. B) The dataset of proteins with a Rep_3 (PF01051) domain (n= 24,824) were combined
656 together with the 1,637 reference Rep_3 (PF01051) proteins from Pfam. The protein sequences with
657 a length of ≥ 40 aa (n=16,930) were aligned using MAFFT. A phylogenetic tree was build using
658 FastTree and visualized using FigTree. A high-resolution version of the phylogenetic tree is available
659 from Figshare at <https://doi.org/10.6084/m9.figshare.14112992>.

660
661 **Figure 3. Comparison of candidate plasmids from global sewage with known plasmids in**

662 **plasmid database (PLSDB).** A) Heat map of centered log ratio (clr)-transformed abundancies of
663 plasmid candidates assigned to plasmids in the PLSDB at bacterial genus level. The phylum level is
664 indicated in parenthesis, A: Actinobacteria; B: Bacteroidetes; aP: alpha-Proteobacteria; bP: beta-
665 Proteobacteria; gP: gamma-Proteobacteria; F: Firmicutes. Clustering of samples was performed using
666 Euclidean distance of the clr-transformed values. B) Principal component analysis of clr-transformed
667 abundancies of known plasmids detected by the PLSDB. The plot on the top reveals similarities and
668 differences between samples. The plot in the bottom reveals the known plasmids that drive the
669 partitioning of the samples, with 17.6% of the variation explained by the first and 11.1% by the
670 second principal component.

672 **Figure 4. Antimicrobial resistance profiles from the whole community and plasmidomes from**
673 **global sewage. A)** Bar plot displaying the proportions of antimicrobial resistance classes detected in
674 a ResFinder-based analysis using the Illumina reads from the whole community, as well as Illumina
675 reads from the plasmid preparations and Nanopore reads from the plasmid preparations. B) Six
676 examples of candidate plasmids are visualized in plasmid maps. The outermost black circle indicates
677 the plasmid chromosome, the coding sequence regions are colored according to their predicted
678 function: replication (blue), mobilization (violet), transposition of DNA (green), antimicrobial
679 resistance (red), toxin-antitoxin systems (orange), hypothetical proteins (hp) and other proteins
680 (grey). The blue and green line indicate the GC and AT-content, respectively. The plasmids are
681 named according to their origin, CIV (Côte d'Ivoire), POL (Poland), USA.1 (USA), BRA (Brasil),
682 CZE (Czechia), and IND (India). Some sequencing errors might still be present in the candidate
683 plasmid sequences, which are likely the reason why a few open reading frames are not properly
684 predicted and appear fragmented, such as the gene encoding for AmpC and Macrolide efflux pump
685 genes in the plasmid from Czechia. A detailed description about the plasmids is available from
686 Figshare at <https://doi.org/10.6084/m9.figshare.14039390>.

687 **Table S1.** Sewage sample information.
688

689 **Figure S1: Length of nanopore sequencing reads.** The violin plot displays log transformed read
690 lengths. The horizontal dashed lines indicate log values for 1.000 and 10.000 bases length,
691 respectively. Most reads exhibit a read length below 10.000 bases, which is the cut-off value for our
692 assembly workflow, and most of the reads are between 1.000 and 10.000 bases long.
693

694 **Figure S2. Plasmid and virus (phage)-related circular DNA elements.** The bar plots display the
695 fraction (A) and total counts (B) of circular contigs containing Pfam IDs specific for plasmid and
696 virus/phage -related proteins per sample. Each predicted protein by prodigal was searched against the
697 pfam databases using HMMER hmmscan and filtered for a p-value less than 0.00001. In a small
698 subset of assemblies we identify both viral and plasmid associated genes. Pfam ID's classified as
699 "other than plasmid & viral" might still be plasmid relevant; they are just not specified as plasmid-
700 related based on the stringent scheme used.
701

702 **Figure S3. Comparison to known plasmids in plasmid database (PLSDB) – clustering on**
703 **individual plasmid level.** Samples with less than 100 circular assembled contigs were removed from
704 the analysis as well as plasmids with less than 10 occurrences over all samples. Clustering of samples
705 (columns) was done using Euclidean distance of the centered log ratio (clr)-transformed values.

706

707 **Figure S4. Comparison between plasmidome samples – MASH distances.** All plasmid candidate
708 sequences for each sample from the five examined continents were sketched using MASH, distances
709 calculated, and visualized by principal component analysis. A) This plot displays the differences and
710 similarities between all 24 plasmidome samples. B) This plot displays the differences and similarities
711 between 22 plasmidome samples (all samples, except NGA and BRA.2).

712

713 **Figure S5. Heatmaps depicting antimicrobial resistance profiles from the whole community
714 and plasmidomes from global sewage** based on presence/absence (A) and centered log ratio (clr)-
715 transformed abundancies (B) of antimicrobial resistance gene classes. The antimicrobial resistance
716 genes were identified in a ResFinder-based analysis using the Illumina reads from the whole
717 community, Illumina reads from the plasmid preparations, and Nanopore reads from the plasmid
718 preparations.

719

720 **Figure S6. Functional characterization of circular DNA elements – GO annotation.** The heat
721 map displays centered log ratio (clr)-transformed abundancies of GO annotations assigned to
722 predicted proteins. Samples with less than 100 circular assembled contig were remove from the
723 analysis as well as GO identifiers with less than 10 occurrences over all samples. The clustering of
724 samples was performed using Euclidean distance of the clr-transformed values resulting in 2 main
725 clusters.

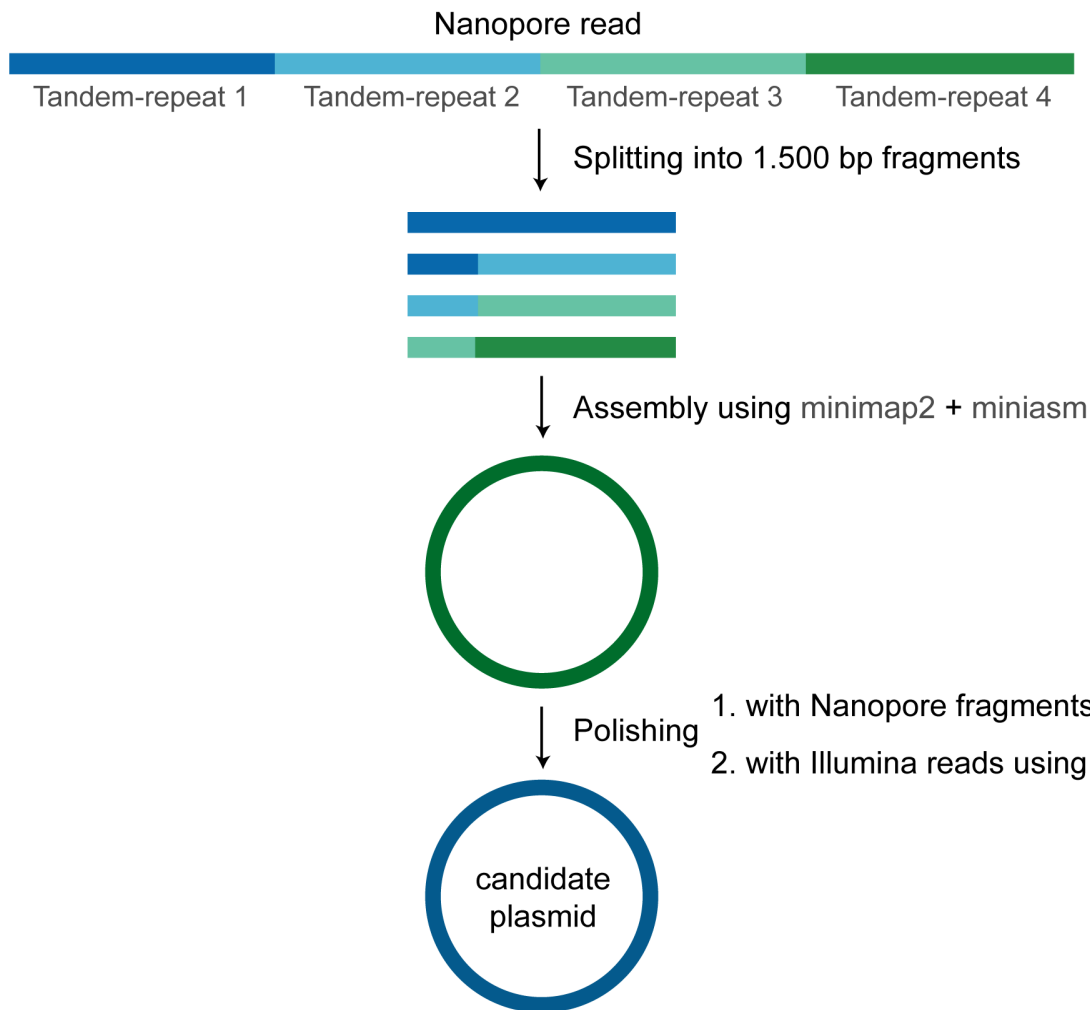
726 **Figure S7. Comparison of AMR genes with prevalence data by CARD**

727 (<https://card.mcmaster.ca>). The most frequently observed AMR genes that were more abundant in
728 plasmidomes (as compared to in the whole community sequencing data) were explored at the CARD
729 website. Here, the prevalence for AMR genes is presented for a selection of pathogens, whether they
730 are associated with the plasmid or chromosome. The prevalence data are calculated as follows:

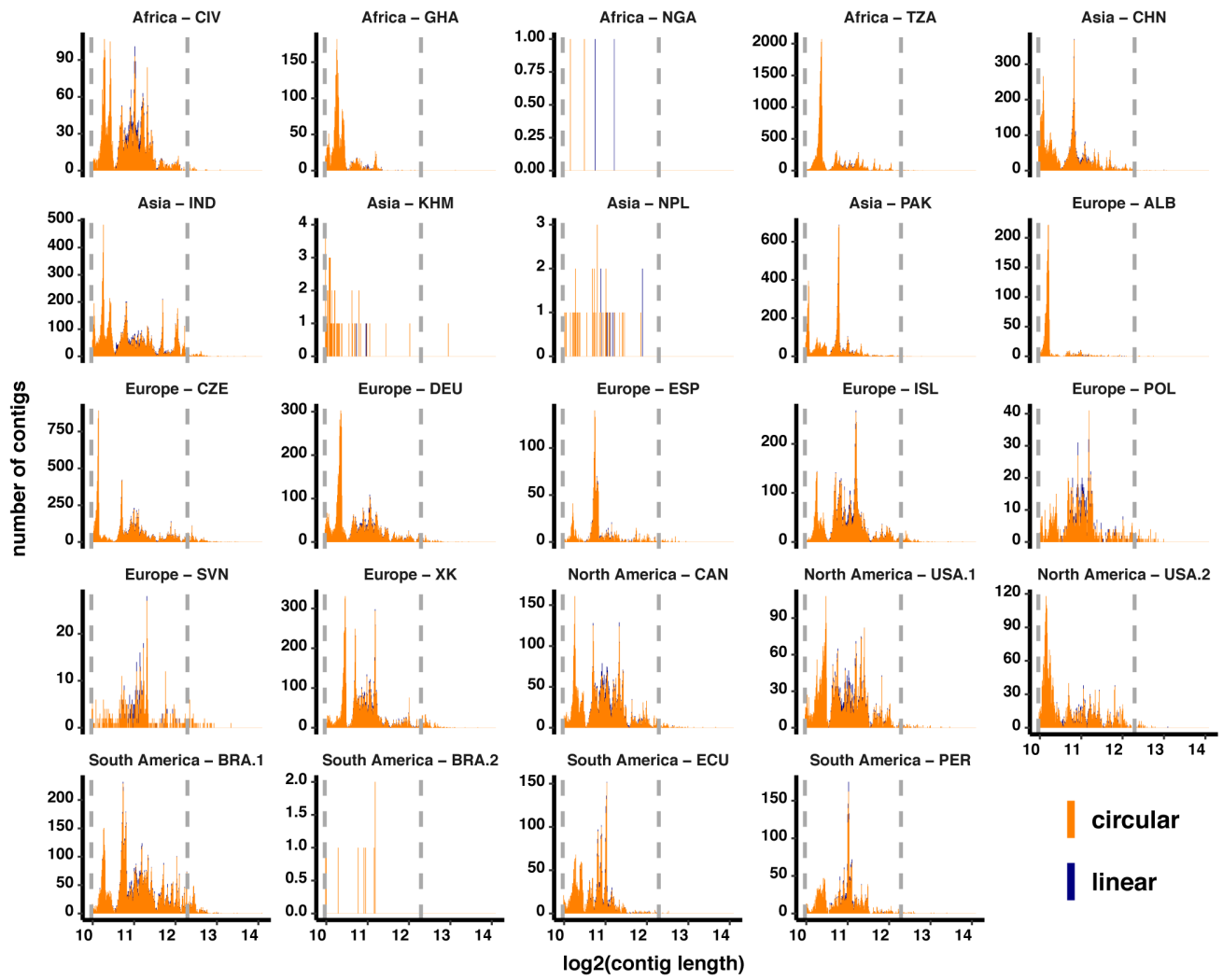
731 Antimicrobial resistance (AMR) molecular prevalence data were generated using the Resistance
732 Gene Identifier (RGI), a tool for putative AMR gene detection from submitted sequence data using
733 the AMR detection models available in CARD. To generate prevalence data, RGI was used to
734 analyze molecular sequence data available in NCBI Genomes for 88 pathogens of interest. For each
735 of these pathogens, complete chromosome sequences, complete plasmid sequences, and whole
736 genome shotgun (WGS) assemblies were analyzed individually by RGI. RGI results were then
737 aggregated to calculate percent occurrence. (See also Alcock *et al.*, NAR, 2020,
738 <https://academic.oup.com/nar/article/48/D1/D517/5608993>).

739

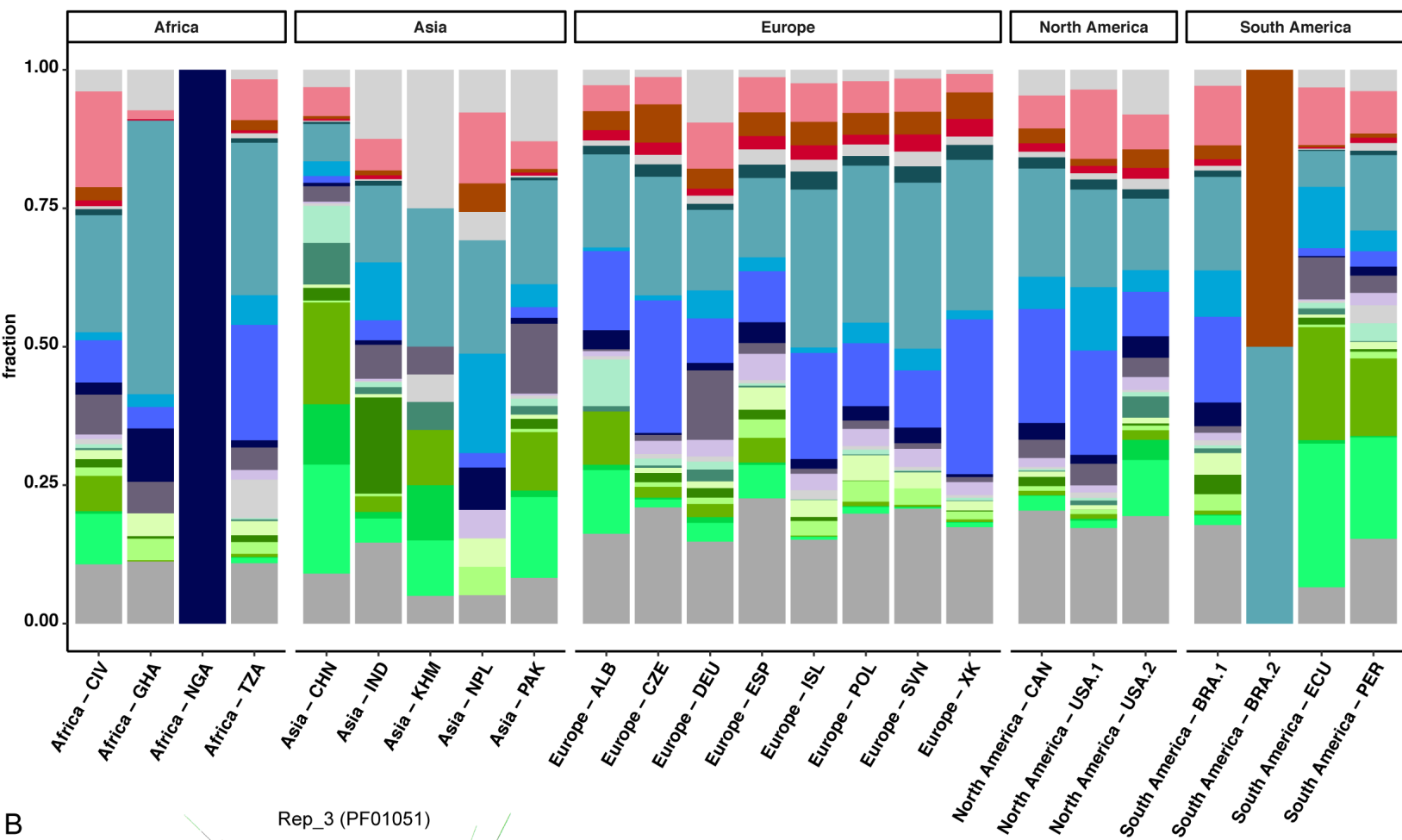
A



B



A



B

